A dynamic model for temperature prediction in a façade-integrated photobioreactor

Eglantine Todisco, Julien Louveau, Charlène Thobie, Emmanuel Dechandol, S. Durécu, Laura Herve, Mariana Titica, Jeremy Pruvost

A dynamic model for temperature prediction in a façade-integrated photobioreactor

E. Todisco[1,2], J. Louveau[1], C. Thobie[1], E. Dechandol[1], L. Hervé[1], M. Titica[1*], J. Pruvost[1]

[1] Université de Nantes, Oniris, CNRS, GEPEA, UMR 6144, F-44600 Saint-Nazaire, France

[2] Séché Environnement, Centre R&D, 1425 Avenue Charles de Gaulle, PIPA, 01150 Saint-Vulbas, France

* Author to whom correspondence should be addressed

Email: mariana.titica@univ-nantes.fr

Key words: Thermal modeling, Photobioreactor, Building facade, Solar, Microalgae

Highlights

- A thermal biofaçade model was developed and validated over 5 months' operation
- A sensitivity analysis revealed the main parameters influencing thermal behavior
- Various temperature regulation pre-set and biofaçade configurations were tested
- A thermal symbiosis between the PBR and the host building proved efficient for temperature regulation
- The introduction of an active passageway enabled significant energy savings

Abstract

There are certain advantages in applying an airlift photobioreactor (PBR) intended for microalgae culture to a building façade, such as making use of the solar illuminated surfaces and the possibility of chemical recycling through photosynthetic growth (utilizing the carbon dioxide emissions from boiler combustion, for example).

This study concerns the development of a thermal model for integral building-façade photobioreactors which can predict dynamic changes in the temperature of the culture medium in response to changes in meteorological conditions, taking into account the thermal interchange with the host building. The proposed model was experimentally validated with data obtained in outdoor conditions, using a pilot-scale system (SymBiO_2-Box) located in Saint-Nazaire (France), and subsequently used to set up numerical simulations and optimization studies to develop control strategies for efficient thermal regulation of the PBR with optimal energy consumption. The

advantage of using an active passageway between the façade and PBRs was investigated in particular.

1- Introduction

Many studies in recent years have been based on the cultivation of microalgae or cyanobacteria, due to their high industrial potential in various applications (energy, green chemistry, food supplements) [1]. Microalgae culture requires water, light, carbon dioxide (CO_2) and nutrients such as phosphorus and nitrogen [2]. Under solar conditions, thermal regulation is often required to maintain suitable temperature conditions for growth [3], with temperature regimes that depend heavily on the cultivation system [4]–[8].

Although a wide variety of systems is available, two main designs can be identified: open systems and closed systems, both having advantages and disadvantages [9]. In terms of thermal regulation, open systems, which are subject to evaporation, require less energy to be maintained at the optimal temperature for algae [8]. However, they also have drawbacks: productivity and biomass quality are usually lower [9]. Intensive culture in closed systems (PBRs) allows for better control of culture conditions, so that growth performance depends only on the light radiation received [4], [10]. However, as a closed geometry, PBRs tend to overheat and temperature regulation can become a critical issue [11].

Each different species has an optimum temperature for growth; moving away from this optimum, productivity decreases and can lead to cell death [12]–[15]. The optimum growth temperature for microalgae is generally between 20° and 25°C, although it depends largely on the species [16]. Most species can tolerate temperatures of between 15° and 30°C. Below 15°C growth slows down, while temperatures above 35°C are lethal to a large number of species [17].

As an initial assumption, the culture composed of microalgae cells and culture medium is considered to absorb almost the entire solar spectrum, depending on the biomass concentration. Infrared is largely absorbed by water and is mainly responsible for the rise in culture temperature, while ultraviolet is absorbed by the glass [18]. In addition, the photosynthesis yield is about 6 - 8% under direct solar irradiation, demonstrating that much of the energy captured in the photosynthetically active radiation (PAR) is lost as heat through exoenergetic biochemical reactions [19]. It is therefore reported that around 95% of the total light spectrum energy captured is converted into heat [20]. Hence, outdoor closed PBRs tend to overheat.

As a consequence, keeping the temperature constant in a PBR can require large amounts of energy, as well as a smart and reactive thermal regulation system. Without regulation, PBRs operated in outdoor solar conditions can easily reach lethal temperatures in any season [18]. It has been

demonstrated that temperatures can be 10° - 30°C higher than the ambient temperature in a closed PBR [17]. On the other hand, morning temperatures can be 10°C below the optimal growth temperature, leading to a low photosynthetic rate over the first few hours of the day [12]. Due to the effect that low temperatures have on cell division, it has also been shown that low night-time temperatures can influence daytime biomass productivity and produce a lower decay rate at night [12], [21].

To reduce the energy costs related to temperature regulation in closed PBRs, it is proposed that microalgae culture in an airlift PBR could be integrated with a host façade. In addition to sharing some of the construction and maintenance costs [20], creating interactions could benefit both the host building and the microalgae culture. Chemical and thermal symbioses are proposed [20], [22], [23]. Chemical symbiosis can be achieved using CO_2 emissions from factories, for example, or from boiler combustion in the host building itself, to grow microalgae through photosynthesis [24]. Thermal symbiosis can be achieved by optimizing thermal exchanges between the host building and the integrated biofaçade PBRs.

This work focuses on optimizing thermal symbiosis. The process is highly dynamic due to the changeable outdoor conditions, and thermal behavior is also a complex result of integrating the PBR geometry with the building architecture. Optimization is therefore not straightforward.

A mathematical thermal model was developed with the aim of developing control strategies derived from integrating the PBR with the façade, and to ensure the best compromise between biomass productivity and energy consumption. A model of this type is highly dependent on the culture system geometry. Various models were found in the literature [3], [5], [6], [25]–[31], but none of them was specific enough for application with biofaçades; these models are able to predict temperature evolution under solar conditions in open pond PBRs [5], [27], [31] and very thin horizontal PBRs [6]. Based on such a model, economically viable solutions for temperature regulation problem in open pond PBRs are proposed in [32]. The approach taken also depends on the environment, especially when it is integrated with a sub-system such as a host building.

This paper addresses the development of a dynamic model able to predict the evolution of the temperature culture medium in a PBR system integrated with a building façade, depending on its overall configuration and the external environmental conditions. It investigates the SymBiO_2-Box, a semi-industrial prototype on which experimental data has been collected at different seasons. The paper describes in detail the mathematical model and related parameters. An experimental validation with the SymBiO_2-Box is then presented. Finally, the discussion focuses on the use of the thermal model to predict energy needs in various thermal regulation strategies.

2- Materials and methods

2-1 SymbiO$_2$-Box

2-1-1 Experiment set-up

Experiments were conducted on SymbiO$_2$-Box pilot-scale prototype representing a biofaçade (Figure 1), installed on the Algosolis R&D facility (Saint-Nazaire, France, 47.2515N -2.2596W). The SymBiO$_2$-Box allows investigation under actual operating conditions to produce data for modeling purposes, for example, as in the present study. It also allows testing of optimized culture strategies prior to implementation on a larger scale. It comprises the following elements:

- Two photobioreactors of flat-panel type composed of a glass optical surface on the front and a steel plate on the back, delimiting the culture volume.
- A protection window in direct contact with the exterior, separated from the PBR optical surface by a thin air layer (AL).
- An air cooling channel (ACC): a passageway that can be closed or opened by automated shutters to modify thermal exchanges with the host building (see below). The ACC also provides access for PBR maintenance.
- The host building, isolated from the culture, with rooms designed to represent the thermal inertia of an actual building.

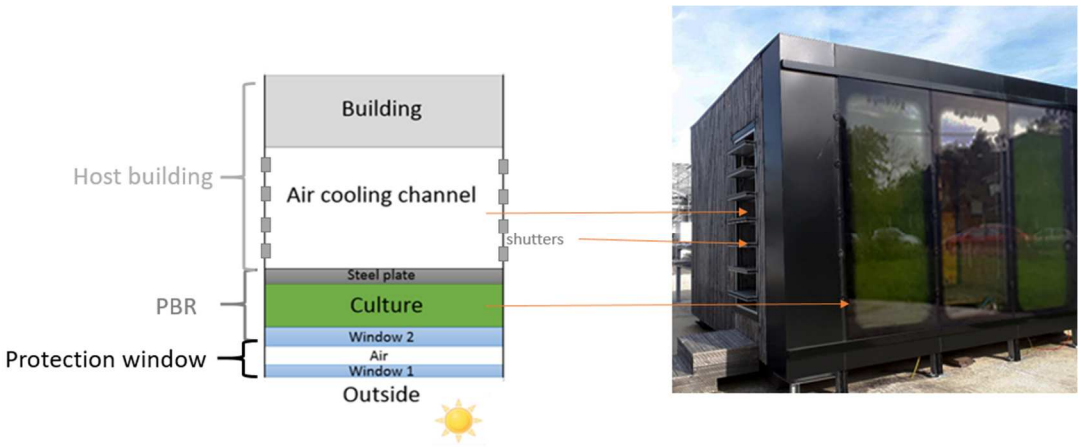

Figure 1 SymBiO2-Box, a pilot-scale biofaçade. On the left view is a schematic drawing from the top, on the right is a picture from the front. The SymBiO2-Box is located in AlgoSolis R&D facility (www.algosolis.com) in Saint-Nazaire, France, facing south. The shutters are used to allow airflow in the air cooling channel and can be seen on the side of the SymBiO$_2$-Box.

2-1-2 Online measurement and data acquisition system

A weather station (Vantage Pro 2, Davis, USA) was used to measure the outside air temperature [°C], global radiation [W.m^{-2}], wind speed [m.s^{-1}] and direction, and relative air humidity (RH) [%]. The sensor was vertically oriented towards the south, parallel to the PBR's optical surface. All data was collected in a text file and input to the thermal model (details below).

K-type thermocouple probes were installed at different points in the SymBiO_2-Box to measure the temperature of the steel plate, the ACC and the water circulating in the double jacket for thermal regulation of the culture. The temperature in the culture was monitored with a pH probe (InPRO 4800i SG 120/M300, Mettler Toledo, Germany), which was also used for pH regulation (M300 multiple channel transmitter Mettler Toledo, Germany). Signals collected from bench components (temperatures and pH) were captured on a computer uploaded with the pilot program developed using LabVIEW® (Laboratory Virtual Instrument Engineering Workbench) control software.

The opening/closing of the ACC was controlled via the software within a programmable range for measuring various temperatures: the ACC, the culture temperature and the building temperature.

2-2 Experiment protocol

Various experiments were carried out to find the best way of collecting data for thermal modeling and subsequent analysis. The first set of data was collected by adding black indian ink to the water to mimic microalgae culture light absorption (close to a black body). Two different conditions were tested: with the ACC constantly closed (May 5th to May 10th 2017) or constantly open (May 10th to May 26th 2017). In a second experiment, the microalgae *Chlorella vulgaris* (CCAP 211/19) was cultivated from November 2017 until April 2018. Different configurations were tested in this 6-month culture period. The ACC was either constantly closed, constantly open, or open only when the culture temperature was above 20°C. It is difficult to maintain a constant temperature in the culture system throughout the day in practice, as the thermal regulation system uses a large amount of power. The benefit of maintaining the culture temperature within a target range was therefore also tested, by defining low and high set points of 15°C and 34°C respectively (see below for more details). This temperature range appeared as a semi-empirical result from the experimental culture campaign as suitable for growing *Chlorella vulgaris* (data not shown). The thermal regulation system was sometimes switched off to let the system evolve freely. Finally, the culture was maintained for a lengthy period between autumn and spring. These combined experiments enabled acquisition of a large set of data based on widely differing weather conditions, which enabled validation of the model for a wide range of weather types (cold and sunny, warm and wet, cold and wet, etc.).

2-3 Thermal modeling

2-3-1 General approach

A model describing thermal exchanges between different components of the system was set up, as described in the section below. This followed a similar approach to the one used by [6], who developed a thermal model for describing the temperature evolution under different operating conditions in a horizontal flat-panel photobioreactor. This model was able to simulate the time

evolution of the culture medium temperature depending on environmental conditions generated by a meteorological database (Meteonorm, www.meteonorm.com).

As with [6] and [8], the system was divided into sub-systems which were modeled through thermal balances. The model is described in the section below.

The black indian ink experiments were used to calibrate the model parameters and verify most of the assumptions. The final validation was carried out using experimental data from microalgae grown in culture condition experiments.

2-3-1 Model hypothesis

- Hypothesis on the culture volume

The culture volume is considered a black body [33]. Ideally, its radiative parameters (absorptivity, transmissivity, reflectivity, emissivity, etc.) should depend on the microalgae concentration [34]. However, these coefficients are difficult to estimate during culture since they also vary according to the culture conditions [6]; light variation, for example, can impact pigment concentration [35]. In this study, this variation was disregarded and constant radiative parameters were used. A similar assumption was made by [6] and [8], assuming an optically dense culture corresponding to a culture concentration in the range 0.5 - 1.5 $kg.m^{-3}$ (expressed here as dry biomass concentration). Note that this condition was verified in practice, as full light attenuation also corresponds to a stable operating regime by preventing over-saturation of cultivated cells with light [20].

Since the PBR was closed, heat loss through evaporation was disregarded.

- Hypothesis on the biofaçade

Because the culture system was particularly shallow compared to its length and width, the thermal model was established assuming a mono-dimensional system [6], [8]. Hence there was no temperature difference between the top of the system and the bottom. Each sub-system, including the photobioreactor, was considered to be of a uniform temperature. The culture volume and the air in the ACC were therefore assumed to be perfectly mixed [6], [36]. In addition, the temperature of the steel plate, the culture medium and the window in contact with the culture were assumed to be equal, due to the efficient thermal exchange between the water and the walls of the PBR. The same assumption was validated by [6] for a flat panel PBR.

All radiative exchanges were assumed to take place in parallel planes. Thus the view factor was always set as equal to 1 [37].

- Hypothesis on gas phases (air)

Air was considered the ideal gas for density calculations. Because the air pressure had shown little variation over a year, the pressure was considered constant and equal to 101 325 Pa (standard conditions). Air density (and therefore the air mass in the ACC) was therefore only affected by temperature. Other characteristics (heat capacity, viscosity) were assumed to be independent of the temperature (values taken at 20°C under atmospheric conditions).

Since air is almost perfectly transparent, its heat absorption was disregarded. Thermal conduction in the air was considered negligible compared to the convection term when calculating heat exchanges with the biofaçade.

Since the air layer in front of the surface of a PBR is very thin, there is very little air mass in it, so temperature variations occur quickly. The temperature of the PBR was therefore taken as the mean of the two sub-systems surrounding it.

When opening the ACC, a natural air flow was created between the building wall and the PBR, with the aim of promoting convection exchanges. The influence of the airflow was then introduced in the model (see the section below). It was assumed that the air in the ACC was of the same hygrometry as the external air. It was also assumed that no air mass accumulation occurred in the ACC. Thus, when it was opened, the air mass entering the ACC was equal to the air mass expelled.

Finally, the heat exchange generated by gas injection into the culture (airlift PBR) was disregarded, unlike other thermal exchanges.

- Hypothesis on the installation and the building

Heat loss can occur through the ACC floor and ceiling due to the thin walls and lack of thermal isolation. Since we used a mono-dimensional system, these losses were not formally modeled with a thermal balance. The quantity of heat lost is also difficult to measure experimentally. A constant heat exchange coefficient was therefore introduced to take heat loss into account; this is identified numerically in the experimental data (see below). This global coefficient was then fixed as a constant and used to calculate heat loss as a function of the temperature difference between the exterior and the ACC. Note that this convection exchange coefficient would certainly vary for different biofaçade designs and would therefore need to be re-calculated.

The ACC being narrow and, in most cases, not aligned with wind direction, the wind speed entering the ACC may be different to the outside speed (the speed measured in our study). An exact representation would require detailed modeling of the fluid dynamics in the ACC, which is outside the scope of this study. As a first assumption, this was represented by semi-empirical modification of the wind speed entering the ACC, as discussed below.

With regard to the building, the temperature was assumed to be homogeneous. The wall separating the building from the ACC was also assumed to be at same temperature as the building's internal walls. Hence, internal radiative exchange between the building walls was not taken into account. In addition, the air movement in the building was considered sufficiently low as to induce no forced convectional heat exchanges. Free convection equations were therefore applied. This hypothesis was implemented in the SymBiO$_2$-Box case, as the building was empty most of the time with the doors kept closed.

2-3-2 Thermal model

As depicted in Figure 2, the system was modeled as four distinct sub-systems: a first sub-system comprising the protection window (subscript w1), a second sub-system formed by the culture (comprising the glass optical window, the actual culture medium and the steel plate on the reverse side of the PBR - subscript culture), a third sub-system formed by the air cooling channel (subscript ACC), and a fourth sub-system formed by the building wall (subscript wall). Like the external (ext) conditions, the building did not represent a subsystem in itself; its temperature represented an input variable in the model.

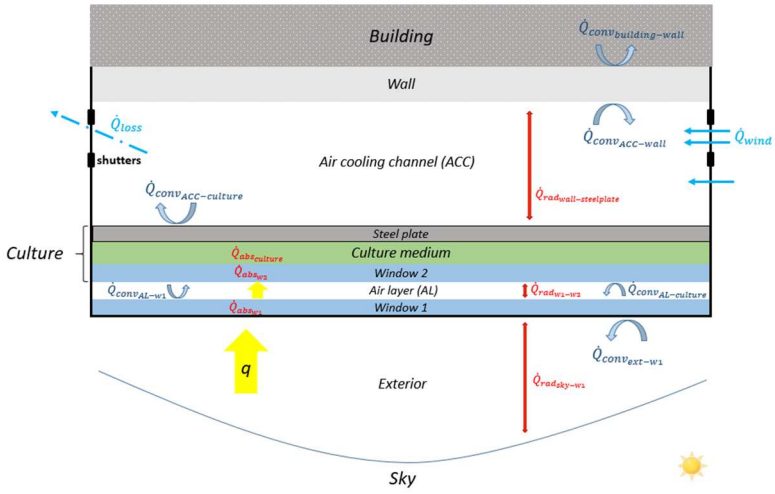

Figure 2 Heat exchanges used in the thermal model. The model divides the system into 4 subsystems : #1 the front window (window 1, subscript w1). #2 the culture medium which includes the second window (subscript w2), the culture medium and the steel plate. #3 the air cooling channel (subscript ACC) and #4 the building wall (subscript wall)

Heat balances describing the thermal behavior of the PBR were carried out from the nodal network defined by the different subsystems (Figure 2). These were obtained by looking at the heat transfers generated by the absorption of solar radiation ($\dot{Q}_{abs}$), convection ($\dot{Q}_{conv}$), radiation ($\dot{Q}_{rad}$), heat loss on the ACC floor and ceiling ($\dot{Q}_{loss}$) and brought about by the wind ($\dot{Q}_{wind}$), and the power added to or removed from the culture medium by the thermal regulation unit ($\dot{Q}_{reg}$). The incident light flux (full solar spectrum) is denoted q [W.m^{-2}].

A heat balance on each sub-system resulted in the following equations:

$$m_{w1} \cdot Cp_{w1} \cdot \frac{dT_{w1}}{dt} = \left(\dot{Q}_{abs_{w1}} + \dot{Q}_{rad_{ext-w1}} + \dot{Q}_{rad_{culture-w1}} + \dot{Q}_{conv_{ext-w1}} + \dot{Q}_{conv_{AL-w1}}\right) \quad \textit{eq. 1}$$

$$(m_{w2} \cdot Cp_{w2} + m_{culture} \cdot Cp_{culture} + m_{steelplate} \cdot Cp_{steelplate}) \cdot \frac{dT_{culture}}{dt} = \left(\dot{Q}_{abs_{w2}} + \dot{Q}_{abs_{culture}} + \dot{Q}_{rad_{w1-w2}} + \dot{Q}_{rad_{wall-steelplate}} + \dot{Q}_{conv_{AL-culture}} + \dot{Q}_{conv_{ACC-culture}} + \dot{Q}_{reg}\right) \quad \textit{eq. 2}$$

$$\rho_{ACC} \cdot V_{ACC} \cdot Cp_{air} \cdot \frac{dT_{ACC}}{dt} = \left(\dot{Q}_{conv_{culture-\mathrm{ACC}}} + \dot{Q}_{conv_{wall-\mathrm{ACC}}} + \dot{Q}_{loss_{ACC}} + \dot{Q}_{wind}\right) \quad \textit{eq. 3}$$

$$m_{wall} \cdot Cp_{wall} \cdot \frac{dT_{wall}}{dt} = \left(\dot{Q}_{conv_{ACC-wall}} + \dot{Q}_{conv_{building-wall}} + \dot{Q}_{rad_{wall-steelplate}}\right) \quad \textit{eq. 4}$$

With $\dot{Q}_{abs_x} = q \cdot \alpha \cdot A_x$ the heat absorption source [37], $\dot{Q}_{rad_{x-y}} = \frac{A_x \cdot \sigma \cdot \left(T_y^4 - T_x^4\right)}{\left(\frac{1}{\epsilon_x} + \frac{1}{\epsilon_y} - 1\right)} = -\dot{Q}_{rad_{y-x}}$ [37] the heat exchanged via radiation and $\dot{Q}_{conv_{x-y}} = h_{x-y} \cdot A_x \cdot \left(T_y - T_x\right) = -\dot{Q}_{conv_{y-x}}$ [37] the heat exchanged by convection. The heat exchange coefficient expression depends on the mode of convection. When free convection applies, the correlation of Churchill and Chu [38] is used $Nu = \left(0.68 + \frac{0.67 \cdot Ra^{\frac{1}{6}}}{\left(1 + \left(\frac{0.492}{Pr}\right)^{\frac{9}{16}}\right)^{\frac{8}{27}}}\right)^2 = \frac{h_{x-y} \cdot Lc}{k}$, here, the characteristic length is the height of the subsystem considered. When the wind blows over the surface of the subsystem, the Mac Adams and Woretz [39] correlation is used $h_{xy} = 5.7 + 3.8 \cdot U_{wind}$. Finally, the heat exchange due to air flow in the ACC is expressed as: $\dot{Q}_{wind-\mathrm{ACC}} = \rho_{\mathrm{air-ext}} \cdot U_{wind-ACC} \cdot S_{shutters} \cdot Cp_{air} \cdot (T_{ext} - T_{ACC})$.

Adimensional numbers equations, geometrical constants, physical properties of the system and additional physical constants are given in supplementary material. Additional parameters and model improvement

To improve the quality of model predictions, the following considerations were introduced for better representation of the influence of the ACC on the overall system.

The presented model is mono-dimensional, therefore, heat losses that occur through the ceiling and the floor are not formally expressed in heat balances. This resulted in noticeable differences between the predicted and measured values during the model validation process (see below). To account this issue, a heat loss term [W] was added to represent those losses. It has been designed as proportional to the difference between ACC temperature and the exterior, the proportional coefficient being F_{loss} [$W.K^{-1}$] :

$$\dot{Q}_{loss_{ACC}} = F_{loss} \cdot (T_{ext} - T_{ACC}) \qquad \text{eq. 5}$$

where F_{loss} is a parameter numerically determined from experimental data, by using an identification procedure presented in the next section.

Similarly, a correction factor was introduced to represent the actual speed of the air flow in the ACC, and then consider where this speed was lower than the wind speed measured outside. This was obtained by introducing a correction factor F_{wind}.

The two empirical parameters have been identified from the experimental data using two different datasets. The first one includes 115 measurements (from May 5th to May 10th) where the ACC was kept closed to estimate Floss. The second one includes 375 measurements (from May 10th to May 25th) with the ACC always open to estimate Fwind. The value of those parameters was optimized by the function fminsearch from MATLAB® software with the Mean Absolute Error (MAE, see below) of the ACC temperature as the criterion to be minimized. The optimized value was finally rounded 3 decimal places. A value of 4.000 W.K-1 and 0.025 was obtained for Floss and Fwind respectively. The parameter's values were finally validated using two other datasets with 1318 *(January 26thto March 22nd; ACC closed) and 654 (March 24th to April 25th; ACC opened) data points respectively.*

In the following, these parameters, which are dependent of the biofaçade design, were then set as constant for the rest of the study.

2-3-3 Model inputs

Meteorological input data (solar radiation, wind speed, exterior ambient temperature and air humidity) were recorded during the experiments (see model validation), or sourced from the meteorological database (simulation section). In the latter case, weather data averaged over the previous 10 years in Nantes (47° 13' 6.136" N 1° 33' 13.036" W, France) were taken from a weather database [40]. Note that q is the total radiation, i.e. the sum of direct and diffuse solar radiation.

2-4 Indicators of model prediction efficiency

In addition to visual inspection, four indicators were used to judge the accuracy of the model prediction [41], [42]. This corresponds to the mean absolute error (MAE), the mean squared error

(MSE), the mean absolute percentage error (MAPE) and the Nash-Sutcliffe efficiency (NSE). These were calculated as shown in Table 2.

Table 1 Statistical indicators and their equations used to assess the validity of the model

Indicator	**MAE** **Mean absolute error**	**MSE** **Mean squared error**	**MAPE** **Mean absolute percentage error**	**NSE** **Nash-Sutcliffe efficiency**
Equation	$MAE = \frac{\sum_i^n \lvert e_i \rvert}{n}$	$MSE = \frac{\sum_i^n e_i^2}{n}$	$MAPE = 100 \cdot \frac{\sum_i^n \frac{\lvert e_i \rvert}{Y_{mes_i}}}{n}$	$NSE = 100 . \left(1 - \frac{\sum_i^n e_i^2}{\sum_i^n \left(Y_{mes} - \frac{\sum_j^n Y_{mes_j}}{n} \right)} \right)$
Where $e_i = Y_{model_i} - Y_{mes_i}$ is the difference between the temperature predicted and the temperature measured at a given time step, and n, the number of values compared				

The MAE indicates the average prediction error of the model and is considered in conjunction with the MSE. A low MAE value with a high MSE value indicates that the model is good on average but produces significant errors for some specific isolated points. The MAPE indicates the error percentage compared to the experimental measurements, while the NSE is a measurement of the 'predictive power of the model' [43], i.e. how the model fits with the experimental data. Its value ranges from -∞ to 1; 1 being a perfect fit between the model and the data and 0 indicating that the model predictions are as accurate as the mean of the experimental data. The literature suggests that an NSE value of 0.5-0.65 indicates a sufficient model quality [44], [45][44], [45][44], [45][44], [45][44], [45][43], [44][42], [43]. The NSE is sensitive to high values of disparity between the model prediction and the actual experimental values.

2-5 Method for calculation of energy consumption

To provide optimal conditions for microalgae growth, the temperature must be kept within a target operating range, as fixed by the biological requirements of the species [8], so the medium needs to be cooled down and warmed up to maintain a culture temperature within this range. It is also essential to simulate the amount of energy needed for thermal regulation, in order to find the best compromise between temperature regulation and energy expenditure.

Heating and cooling regulation costs were calculated over a year using the model. Infinite power for the thermal regulation unit was assumed (i.e. sufficient power for the system to produce an instantaneous ideal thermal response). Temperature regulation started when the culture medium fell outside the fixed threshold interval.

Because thermal regulation is highly dependent on the target operating range, three temperature intervals were studied: a constant optimal temperature of 23°C, a temperature range between 20°C and 26°C, and a temperature range between 15°C and 34°C. These ranges were retained arbitrarily to calculate the optimal temperature growth for *Chlorella vulgaris* [30], a narrow range variation around the optimal temperature, and a wide range of temperature regulation, respectively.

For each temperature regulation set point, 3 modes of ACC operation were compared: ACC constantly open, ACC constantly closed, and ACC open or closed in accordance with a simple control algorithm reported in Figure 3. This control algorithm was based on culture medium temperature but also took into account the variation in sunlight in a simple way to anticipate the temperature build-ups (i.e. sunrise) and drops (i.e. sunset) that can occur in PBRs; the ACC opened not just when the culture needed to be cooled down but also when the light intensity increased. This was useful, for example, to prevent the ACC opening at the end of the day when the temperature was decreasing and the culture would then need warming up. Similarly, ACC was closed when the culture medium temperature was too low or when the light intensity was decreasing to prevent loss of heat that will be needed during the night.

If culture medium temperature > high value of temperature set-point

➔ Open the ACC

Else if culture medium temperature < low value of temperature set-point

➔ Close the ACC

Else if light input is increasing

➔ Open the ACC

Else

➔ Close the ACC

End

Figure 3 Control algorithm for dynamic ACC

3- Results and discussion

3-1 Thermal model validation

The model was implemented in Matlab® software with parameter values given in supplementary material. Validation was obtained by inputting actual meteorological data registered on the SymBiO_2-Box in the model, and comparing the model predictions first with the experimental temperatures obtained with a façade PBR filled with black indian ink, then on experiments where microalgae were

cultivated in fed-batch mode. These two experimental campaigns were carried out between November 2017 and April 2018 with open and closed ACCs. The influence of the correction factors to better represent the ACC influence was also tested by introducing the correction factors F_{loss} and F_{wind} (eq. 5).

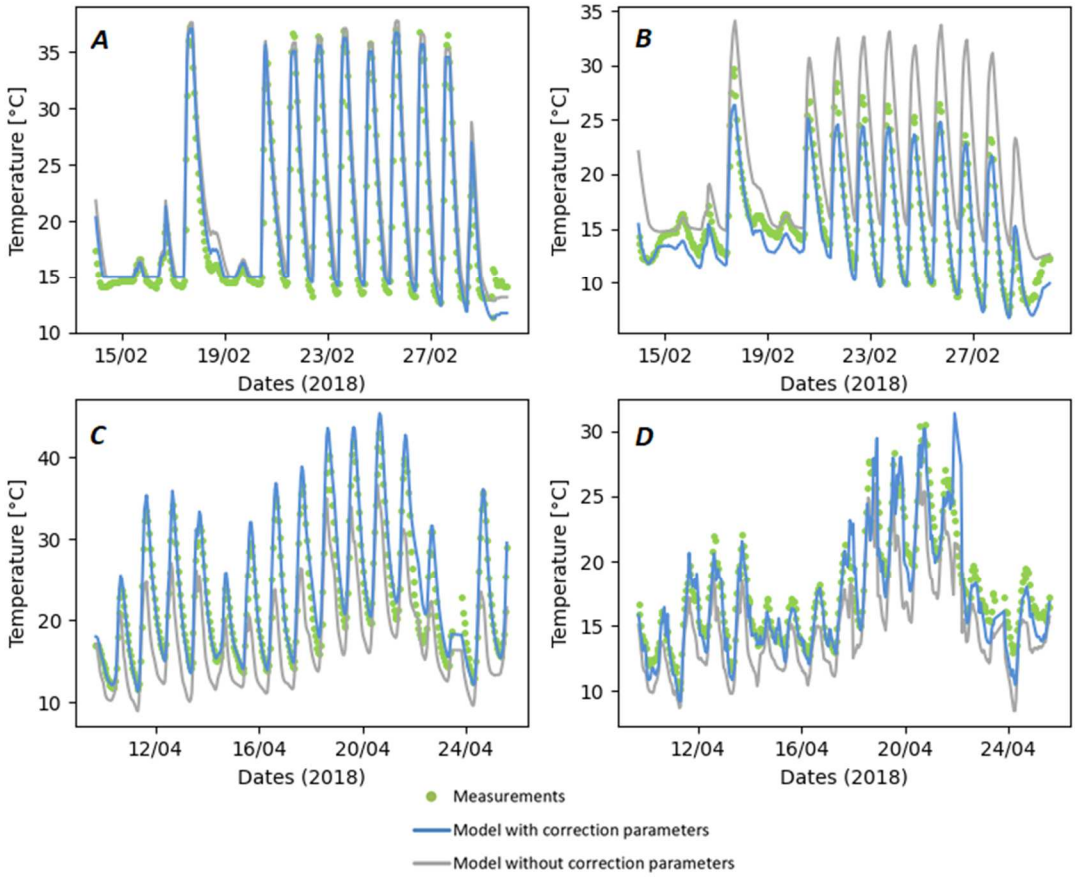

Figure 4 Model validation: Examples of culture medium and ACC temperature evolutions depending on different experimental and weather conditions, with (A) representing the culture temperature when the ACC was kept closed, (B) the ACC temperature with the ACC always closed, (C) the culture temperature when the ACC was kept open, and (D) the ACC temperature with the ACC always open.

Table 2: Validation of the thermal model for various ACC configurations, with and without parameter improvement (see text for details)

Data Set	Culture Medium Temperature				ACC Temperature			
	MAE [°C]	MSE [-]	MAPE [%]	NSE [-]	MAE [°C]	MSE [-]	MAPE [%]	NSE [-]
Closed ACC – indian ink	2.07	5.14	7.95	0.86	5.65	36.78	24.19	0.71
Open ACC – indian ink	4.38	24.91	18.06	0.45	1.45	2.96	8.02	0.80
Closed ACC – indian ink with improved model	0.76	0.93	2.74	0.97	0.93	1.65	3.85	0.87
Open ACC – indian ink with improved model	0.58	0.68	2.47	0.98	0.92	1.67	5.25	0.87
Closed ACC – culture with improved model	1.21	2.38	6.16	0.95	1.24	2.25	7.80	0.91
Open ACC – culture with improved model	0.73	0.99	4.34	0.98	0.84	1.02	6.75	0.97

Figure 4 represents examples of time evolutions of the culture temperature over a period of 12 days (data not fully shown for purposes of readability), and Table 3 summarizes the indicators on model accuracy obtained for each experiment. The graphical comparison between predicted and experimental values in Figure 4 shows that the model was able to reproduce the evolutions observed with an acceptable level of accuracy. The differences between the model with and without correction parameters can also be seen. A systematic underestimation of the temperature evolution was predicted without improving representations of the ACC influence. In all cases, introducing correction parameters led to a more accurate prediction of the culture temperature, as shown in Table 3. This was especially the case when the ACC was open, as can be seen from the model improvement itself, the main purpose of which was to better represent the effect of the airflow inside the open ACC. With model improvement, culture temperature prediction was over 0.95. Note that temperature prediction for the ACC is slightly less accurate but NSE is still close to 0.9.

The resolution with the correction parameters was retained for the rest of the study. However, note that these parameters, which take into account the airflow in the ACC for example, are specific to the experimental set-up and would need to be recalculated for other biofaçade installations. In terms of our results, only two sets of data would therefore be needed - thermal and culture condition - with the ACC respectively open and closed. Note also that the MSE values were already high without model improvement, although the other indicators were generally acceptable. This demonstrates that the model gave good predictions of temperature evolution on average, but with isolated large disparities.

Figure 4 shows sample temperature evolutions obtained for each part of the system, obtained from the improved model. Note that the culture is always the warmest part, and that window 1, which is in contact with the air on the outside, is the coldest. In terms of dynamics, the building wall did not react as quickly as the other system. Figure 5 also shows the evolution of culture temperature over time, ranging from 15°C to over 34°C over a 24 h period (which could be critical for *Chlorella vulgaris*, data not shown). A direct relation with solar light flux is observed here, as the temperature increased during the day then dropped over night. The lowest temperature was around 15°C, although external temperatures could drop below 5°C (close to window 1). This is explained here by the configuration with the ACC closed, which enabled heat absorbed during the day to be retained. Similar behavior can be observed in Figure 4, in the first experiment campaign.

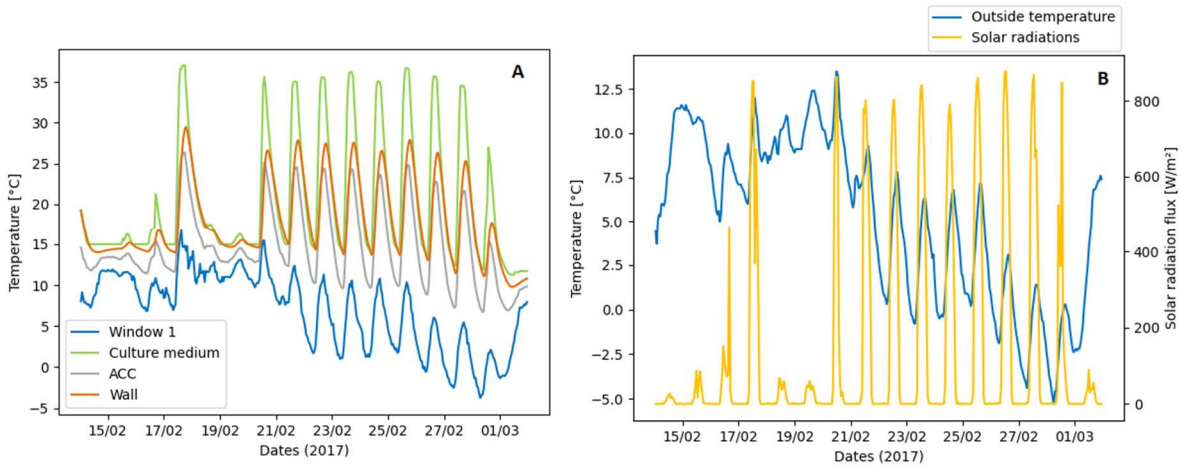

Figure 5 :Model simulation results: A time evolution of temperatures obtained in each sub-system of a biofaçade for the ACC always closed with B outside temperature and solar radiation flux.

3-2 Model behavior and sensitivity analysis

Sensitivity analysis provides important information on the influence that model parameter variations have on model outputs, and the quality of the identification of parameters calibrated on experimental data. This is useful for validation of the model structure. In addition, the properties of the materials and the sensitivity functions in relation to geometry-type parameters provide valuable information for optimizing construction of the system, by identifying which parameters have the most influence on the predicted quantities. A complete sensitivity analysis was computed over the 37 constant parameters of the model. The methodology and the complete results are provided in the supplementary material, only the main outcomes will be discussed here.

We focused our study on predicting the temperature of the culture medium, which is the primary target of our model approach. The sensitivity analysis shows that the most influential parameters are the ones relating to the amount of light absorbed by the culture system. As sunlight is the main heat source for the system, any parameter that modifies its ability to warm the system has an important effect on model prediction. For example, the solar factor of Window 1, which represents the ability of the glass to transmit solar radiation, is shown to be the most important factor during the heating phase. Decreasing solar factor value (e.g. with dust deposition) will reduce the temperature of the culture but will also reduce the amount of light received by the culture and therefore reduce productivity.

Glass emissivity is another important characteristic of the windows, as it represents the amount of heat energy emitted from the glass through radiation. Our sensitivity analysis shows that only the emissivity of window 1 had a non-negligible effect on the culture temperature. This parameter therefore appears in the balance of heat radiation exchanges between window 1 and the exterior,

which acts as a heat sink. So, using a low emissivity window as the first window was shown to be mandatory in our case, to reduce culture heating.

Regarding the factors that were unknown *a priori* and therefore calibrated numerically from the experimental data (i.e. ACC loss factors and ACC wind factor), none were found to be highly sensitive. This tends to validate the model structure.

This sensitivity analysis shows that none of the PBR's parameters exceeded 0.3% model variation/% parameter variation. This can be explained by the weather, for which related parameters were found to be the most influential. Therefore, accurate measurement and estimation of the weather conditions are more important in practice than precise knowledge of other engineering parameters.

3-3 Estimating energy consumption for thermal regulation

To illustrate the impact of different ACC configurations on the temperature of the culture, various simulations were conducted for the same outdoor conditions. The simulated day was January 3, as obtained from a meteorological database (Nantes, France). This day was specially retained as a case study due to the combination of high light received on the PBR surface and low exterior temperature (winter season with clear sky).

The results are given in Figure 5. They illustrate the influence of closing the ACC to reduce cooling of the PBR by the airflow inside. The culture temperatures were higher, almost 10°C more than with the ACC kept open. The effect of introducing dynamic control of the ACC is also demonstrated. In our case, the ACC was open during the day between 10 am and 8 pm, then closed. As shown in Figure 5, this allowed temperature increases and decreases to be limited during the day and night respectively. However, in all cases, the culture medium temperature was largely found to range typically between 10° and 15°C in the morning, and up to 45°C or above at the end of the afternoon. This temperature regime would certainly have impaired biomass growth or even been lethal to the culture. The impact of the ACC together with a thermal regulation between 15° and 34°C is also useful to note; the active thermal regulation allowing good control over the culture temperature, in conjunction with the impact of the ACC. It was observed that the ACC must be closed two hours earlier when using this type of thermal regulation.

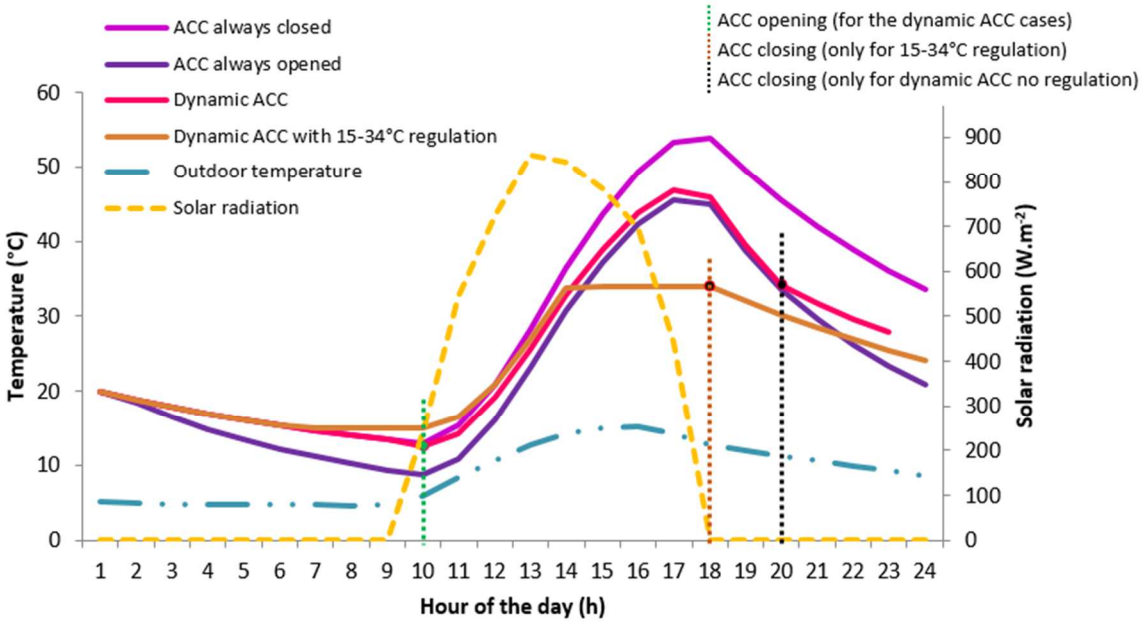

Figure 6 Daily time evolution of the culture medium temperature for various ACC states. The day simulated was the 3rd of January (2018). Vertical lines correspond to the opening of the ACC shutters

The model was then used to simulate various thermal regulation strategies. This was done by adding a heat-sink source term $\dot{Q}_{regul}$ to the thermal balance of the culture [8]:

$$(m_{w2} \cdot \mathrm{Cp_{w2}} + m_{culture} \cdot Cp_{culture} + m_{steelplate} \cdot Cp_{steelplate}) \frac{dT_{culture}}{dt} = \dot{Q}_{regul} + \sum \dot{Heat\ fluxes} \quad \text{eq. 6}$$

In this equation, heat fluxes represent all the absorption and convection fluxes on the culture as detailed in section 2-3-2. $\dot{Q}_{regul}$ is the thermal energy needed to compensate these fluxes, to maintain the culture temperature within the target range. These fluxes can be positive or negative depending on whether the culture needs to be warmed up or cooled down.

Equation 6 allows for simulation of the energy used by an external cooling or heating system designed to maintain the temperature of the culture within the target operating range. As soon as the temperature drifted out of the pre-set range, Equation 6 was applied and the heat-sink source power $\dot{Q}_{regul}$ calculated accordingly. The corresponding energy was then calculated by integrating the power values obtained at all the time steps. Values of energy Q_{regul} were expressed in kWh exchanged over one hour and per PBR.

Note that infinite power was assumed for the thermal regulation unit to estimate the energy needs for thermal regulation. This allowed the culture temperature to be kept within the target operating

range regardless of outdoor conditions, by calculating the instantaneous power to inject or extract in order to keep the temperature constantly within the target range. An actual thermal regulation unit with limited power could easily be incorporated in the model; this would mean, however, that if there was insufficient power, the temperature of the culture could not be maintained within the pre-set range. Infinite power to the thermal unit was assumed here since the objective was to estimate energy requirements. An example of temperature evolution is given in Figure 6 for a temperature interval with thermal regulation set between 15° and 34°C, facilitated by ACC passive regulation.

Figure 7 shows the energy required for thermal regulation units for different pre-set temperature ranges: a constant temperature of 23°C (Figure 7a), temperature ranges of 20° - 26°C (Figure 7b) and 15°- 34°C (Figure 7c), and for different ACC configurations (open, closed and dynamic). Heating and cooling energy requirements were identified.

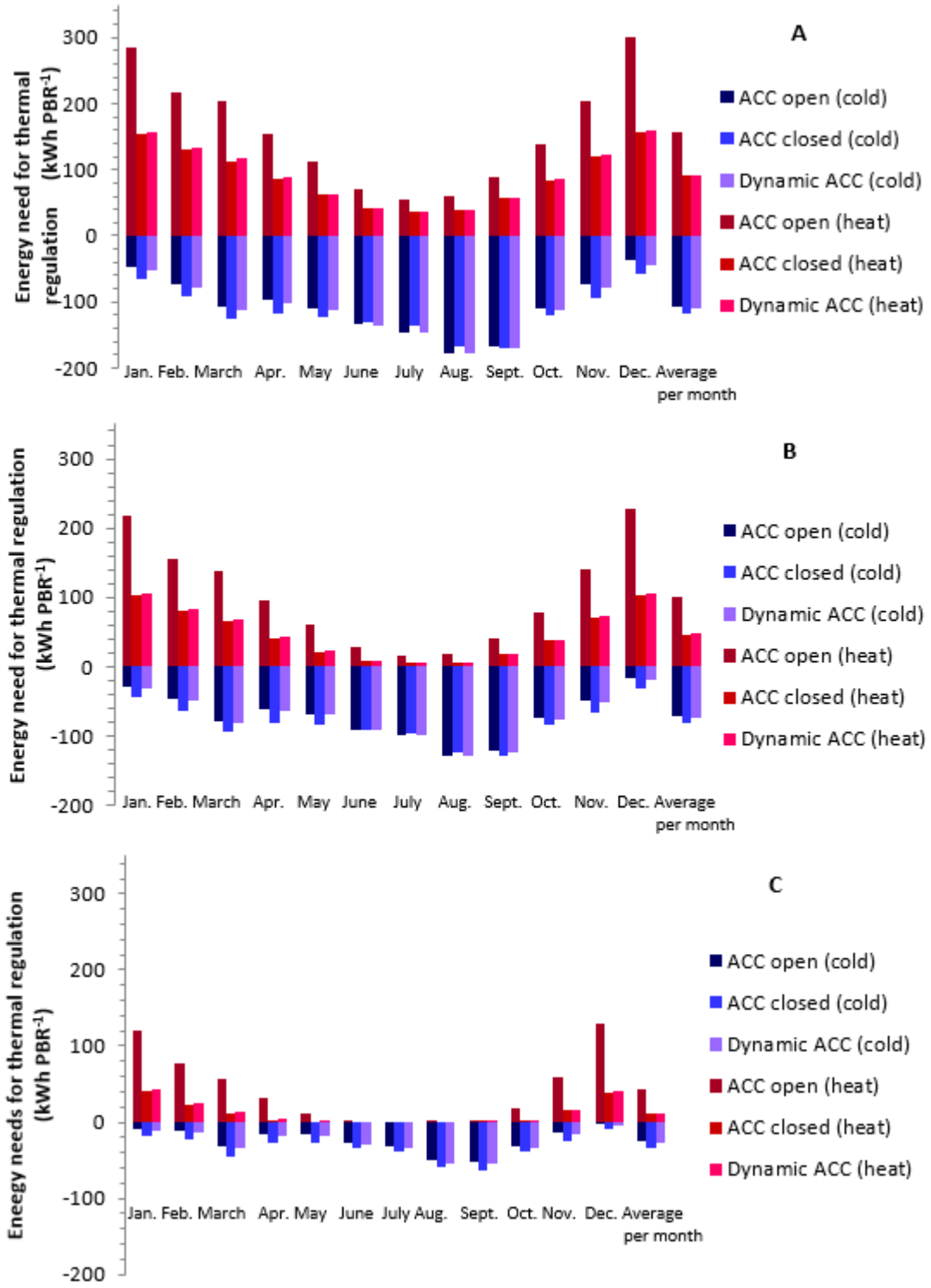

Figure 7 Values of heat energies exchanged for a thermal regulation pre-set at (a) Tculture = 23°C (b) Tculture = [20-26]°C (c) Tculture = [15-34]°C and for various ACC configuration

Simulations confirmed that the energy consumed by thermal regulation increases when the temperature set-point interval is narrower. This appeared to have a major impact: up to five times less energy was consumed with the optimal regulation at a constant temperature of 23°C than in the range 15°-34°C. More to the point, it also showed that the configuration with the ACC constantly open generally required more heating power and less cooling power than with the ACC constantly

closed. Since the outdoor temperatures were lower than the culture temperature, heat exchanges at the back of the PBR tended to reduce the PBR temperature. Using a dynamic ACC led to the same energy requirement for heating as with the ACC closed, and the same cooling energy as with the ACC open. This means that the two ACC configurations can be used to advantage in a given period such as the day (i.e. ACC open to promote heat loss from the PBR) non-sunny daytime periods or night (i.e. ACC closed to prevent too much heat loss during the night). This could easily be automated by linking the opening and closing of the ACC to the light received and sunrise/sunset times. Note that in our case, dynamic regulation of this type suggested the ACC should be opened and closed once or twice a day. In mid-season, action on the ACC shutters could be more frequent due to high solar radiation, low outdoor temperature and changing weather conditions. Note that in terms of energy consumption, shutters have a negligible energy requirement (a few Wh) compared to thermal regulation. Automated shutters appear, therefore, to be a potential solution for reducing the energy required for thermal regulation of PBRs.

Table 3: Summary of monthly averaged energy demands

		23°C	**20-26°C**	**15-34°C**
ACC open (kWh.PBR^{-1})	ACC open (cold)	-106.6	-71.5	-24.3
	ACC open (heat)	157.4	101.6	42.7
	Total ACC open	264.0	173.1	66.9
ACC close (kWh.PBR^{-1})	ACC close (cold)	-116.5	-82.0	-34.0
	ACC close (heat)	90.1	47.0	11.4
	Total ACC close	206.7	129.0	45.4
Dynamic ACC (kWh.PBR^{-1})	Dynamic ACC (cold)	-109.9	-73.5	-26.7
	Dynamic ACC (heat)	91.9	48.5	12.3
	Total dynamic ACC	201.8	122.0	39.0

The average monthly energy requirement was calculated from the total energy consumption over a year, for all configurations. The results are summarized in Table 4. It can be seen that regulation at 20°-26°C or 15°-34°C for any ACC status could save up to 4 - 5 times the energy compared to a constant 23°C setting. This demonstrates the relevance of pre-setting the temperature interval in the thermal regulation strategy. The same conclusion was made in [8]. The ACC configuration was also shown to have an influence. Firstly, it can be noted that an ACC constantly open will lead to higher global energy needs than an ACC that is constantly closed. A dynamic ACC that adapts according to day/night periods saves 1.3 - 1.7 times as much energy, the greatest impact being with the wider 15°

- 34°C range. All the results tended to demonstrate that the ACC could be used to significantly reduce energy requirements for a façade PBR.

In this study, a simple dynamic control based on a day/night cycle was investigated. The development of advanced control strategies, taking into account the dynamic thermal behavior of the overall system (ACC and PBR), could lead to a further decrease in energy needs. This approach would be based on thermal modeling, as in this study, to accurately link outdoor conditions to various aspects that influence the thermal behavior of the façade, such as its ability to absorb light, thermal inertia and exchanges between the building and the PBR through the ACC. This will be the focus of future works that will take into account the time evolutions of external weather conditions and implement an optimized real-time control of the ACC's opening and closing.

4- Conclusion

A thermal dynamic model adapted to microalgae culture in a building façade equipped with an air cooling channel (ACC) was developed and experimentally validated on a pilot-scale system located in Saint-Nazaire (France). An analysis in simulation demonstrated its ability to predict the time evolution of the culture medium temperature. A sensitivity analysis allowed for the importance of certain key parameters, such as front window characteristics (emissivity and solar factor) during the daytime period, and design parameters affecting the overall thermal inertia of the culture system (culture volume, heat capacities of materials).

A wide range of temperature evolutions was found for all configurations, which could be detrimental or even lethal to the microalgae growth. Controlled opening/closing of the ACC with automated shutters proved an efficient solution for limiting temperature variations. The model was then used to predict the energy needs for culture medium temperature regulation at given intervals, and confirmed the ability of the ACC to significantly reduce energy needs over a year's operation, especially when combined with a wide pre-set temperature range.

Future works will aim to determine the effects of various temperature cycles on microalgae culture performance. Advanced control strategies will also be developed for real-time control of the ACC depending on changing meteorological conditions. This will allow for optimal use of the air-cooling channel to optimize the thermal symbiosis with the support building, with the aim of developing a semi-passive thermal regulation system.

5- Acknowledgments

This work was supported by the FUI SYMBIO2 industrial project which aims to develop building façades with integrated photobioreactors for producing microalgae biomass in industrial and urban environments, while inducing symbiotic thermal and chemical exchanges with the support building.

The project involved architects (X-TU), providers of technological solutions for waste treatment (Séché Environnement) and microalgae cultivation (AlgoSource Technologies), metal work specialists for design of the PBR (Viry), specialists in energy and environmental building integration (Oasiis, LHEEA), and an expert academic partner in PBR engineering (GEPEA, UMR CNRS).

6- Abbreviations

Latin letters

A	Area [m^2]
Cp	Heat capacity [$J.kg^{-1}.K^{-1}$]
d	Density [$kg.m^{-3}$]
dvf	Dead volume fraction of the ACC [-]
e_i	Difference between predicted and measured temperature
F_{loss}	Heat loss coefficient [$W.K^{-1}$]
Fs	Solar fraction [-]
g	Gravitational acceleration [$m.s^{-2}$]
Gr	Grashof number [-]
h	Convection coefficient [$W.m^{-2}.K^{-1}$]
H	Height [m]
k	Conduction coefficient [W.m-2.K-1]
Lc	Characteristics length [m]
m	mass [kg]
M	Molar mass [$kg.mol^{-1}$]
$\dot{m}$	Mass flow [$kg.s^{-1}$]
n	Number of values
Nu	Nusselt number [-]
P	Pressure [Pa]
Pr	Prandt number [-]
q	Incident light [$W.m^{-2}$]
$\dot{Q}$	Heat exchanges [W]
r	Mass fraction of water in the air [-]
R	Ideal gas constant [$J.mol^{-1}.K^{-1}$]
Ra	Rayleigh number [-]
S	Sensitivity function [-]
T	Temperature (K)
t	Time [s]
U	Speed [$m.s^{-1}$]
V	Volume [m^3]
ƶ	Staggering coefficient [degree]

Greek letters

µ	Dynamic viscosity [$kg.m^{-1}.s^{-1}$]
ε	Emissivity [-]
α	Absorptivity [-]
β	Dilatation coefficient [K^{-1}]
θ	Wind direction [degree]
σ	Stephan-Boltzman constant [$W.m^{-2}.K^{-4}$]
υ	Kinematic viscosity [$m^3.s^{-1}$]

Subscripts

abs	Heat absorption
w1	Window 1
AL	Air Layer
wall	Building wall
conv	Heat exchanged by convection
ext	Laboratory Virtual Instrument Engineering Workbench
lat	latent
rad	Heat exchanged by radiations
reg	Thermal regulation
sat	Saturation
vap	Vapor

Acronyms

MAE	Mean Absolute Error
MAPE	Mean Absolute Percentage Error
MSE	Mean squared error
NSE	Nash Sutcliffe efficiency
PAR	Photosynthetically active region
PBR	Photobioreactor
LabVIEW	Laboratory Virtual Instrument Engineering Workbench
ACC	Air Colling Channel

Units

[°C]	Degrees Celsius
[h]	Hour
[J]	Joule
[K]	Degrees Kelvin
[kg]	Kilogram
[m]	Meter
[mol]	Mole
[Pa]	Pascal
[s]	Second
[W]	Watt

χ_{wind} Wind speed correction factor [-]

7- References

[1] J. J. Milledge, « Commercial application of microalgae other than as biofuels: a brief review », *Rev. Environ. Sci. Biotechnol.*, vol. 10, n° 1, p. 31-41, mars 2011, doi: 10.1007/s11157-010-9214-7.

[2] Clemens. Posten et C. Walter, *Microalgal Biotechnology: Potential and Production*. 2012. doi: 10.1515/9783110225020.

[3] O. Bernard et B. Rémond, « Validation of a simple model accounting for light and temperature effect on microalgal growth », *Bioresour. Technol.*, vol. 123, p. 520-527, 2012, doi: 10.1016/j.biortech.2012.07.022.

[4] J. Pruvost, J. F. Cornet, F. Le Borgne, V. Goetz, et J. Legrand, « Theoretical investigation of microalgae culture in the light changing conditions of solar photobioreactor production and comparison with cyanobacteria », *Algal Res.*, vol. 10, n° 3, p. 87-99, 2015, doi: 10.1016/j.algal.2015.04.005.

[5] M. Huesemann *et al.*, « A validated model to predict microalgae growth in outdoor pond cultures subjected to fluctuating light intensities and water temperatures », *Algal Res.*, vol. 13, p. 195-206, 2016, doi: 10.1016/j.algal.2015.11.008.

[6] V. Goetz, F. Le Borgne, J. Pruvost, G. Plantard, et J. Legrand, « A generic temperature model for solar photobioreactors », *Chem. Eng. J.*, vol. 175, n° 1, p. 443-449, 2011, doi: 10.1016/j.cej.2011.09.052.

[7] J. Pruvost, J. F. Cornet, V. Goetz, et J. Legrand, « Modeling dynamic functioning of rectangular photobioreactors in solar conditions », *AIChE J.*, vol. 57, n° 7, p. 1947-1960, juill. 2011, doi: 10.1002/aic.12389.

[8] J. Pruvost, V. Goetz, A. Artu, P. Das, et H. Al Jabri, « Thermal modeling and optimization of microalgal biomass production in the harsh desert conditions of State of Qatar », *Algal Res.*, vol. 38, n° November 2018, p. 101381, 2019, doi: 10.1016/j.algal.2018.12.006.

[9] M. R. Tredici, « Mass Production of Microalage : Photobioreactors », in *Handbook of Microalgal Culture: Biotechnology and Applied Phycology*, 1st éd., A. Richmond, Éd. Oxford: Blackwell Science, 2004, p. 178-214. doi: 10.1002/9780470995280.

[10] A. P. Carvalho, S. O. Silva, J. M. Baptista, et F. X. Malcata, « Light requirements in microalgal photobioreactors: an overview of biophotonic aspects », *Appl. Microbiol. Biotechnol.*, vol. 89, n° 5, p. 1275-1288, mars 2011, doi: 10.1007/s00253-010-3047-8.

[11] A. P. Carvalho et L. A. Meireles, « Microalgae reactors: A review of enclosed systems and performances », *Biotechnol. Prog.*, vol. 3, n° 1, p. 1490-1506, 2006.

[12] G. Torzillo, A. Sacchi, et R. Materassi, « Temperature as an Important Factor Affecting Productivity and Night Biomass Loss in Spirulina platensis Grown Outdoors in Tubular Photobioreactors », *Bioresour. Technol.*, vol. 38, p. 95-100, 1991, doi: 10.1016/0960-8524(91)90137-9.

[13] Md. Rafiqul Islam, A. Hassan, G. Sulebele, C. Orosco, et P. Roustaian, « Influence of temperature on growth and biochemical composition of Spirulina platensis and S. fusiformis », vol. 4, n° 2, p. 97-106, 2003.

[14] A. Converti, A. A. Casazza, E. Y. Ortiz, P. Perego, et M. Del Borghi, « Effect of temperature and nitrogen concentration on the growth and lipid content of Nannochloropsis oculata and Chlorella vulgaris for biodiesel production », *Chem. Eng. Process. Process Intensif.*, vol. 48, n° 6, p. 1146-1151, 2009, doi: 10.1016/j.cep.2009.03.006.

[15] J. Pruvost, J. Cornet, et L. Pilon, « Large-Scale Production of Algal Biomass : Photobioreactors », p. 41-66, 2016, doi: 10.1007/978-3-319-12334-9.

[16] J. P. Bitog *et al.*, « Application of computational fluid dynamics for modeling and designing photobioreactors for microalgae production: A review », *Comput. Electron. Agric.*, vol. 76, n° 2, p. 131-147, 2011, doi: 10.1016/j.compag.2011.01.015.

[17] T. H. Mehlitz, « Temperature Influence and Heat Management Requirements of Microalgae Cultivation in Photobioreactors », n° February 2009, p. 152, 2009, doi: 10.15368/theses.2009.15.
[18] F. Le Borgne, « Développement d'un photobioréacteur solaire intensifié en vue de la production à grande échelle de biomasse microalgale », Université de Nantes, 2011.
[19] J. Cornet, « Procédés limités par le transfert de rayonnement en milieu hétérogène », Habilitation à diriger des recherches, Université Blaise Pascal - Clermont-Ferrand II, 2007.
[20] J. Pruvost, B. Le Gouic, O. Lepine, J. Legrand, et F. Le Borgne, « Microalgae culture in building-integrated photobioreactors: Biomass production modelling and energetic analysis », *Chem. Eng. J.*, vol. 284, p. 850-861, 2015, doi: 10.1016/j.cej.2015.08.118.
[21] F. Le Borgne et J. Pruvost, « Investigation and modeling of biomass decay rate in the dark and its potential influence on net productivity of solar photobioreactors for microalga Chlamydomonas reinhardtii and cyanobacterium Arthrospira platensis », *Bioresour. Technol.*, vol. 138, p. 271-276, 2013, doi: 10.1016/j.biortech.2013.03.056.
[22] J. Pruvost, B. L. E. Gouic, O. Lepine, J. Legrand, et F. L. E. Borgne, « Symbiotic Integration of Photobioreactors in a Factory Building Façade for Mutual Benefit Between Buildings and Microalgae Needs », n° April, 2014.
[23] G. M. Elrayies, « Microalgae: Prospects for greener future buildings », *Renew. Sustain. Energy Rev.*, vol. 81, n° August 2017, p. 1175-1191, 2018, doi: 10.1016/j.rser.2017.08.032.
[24] S. A. Razzak, M. M. Hossain, R. A. Lucky, A. S. Bassi, et H. De Lasa, « Integrated CO2capture, wastewater treatment and biofuel production by microalgae culturing - A review », *Renew. Sustain. Energy Rev.*, vol. 27, p. 622-653, 2013, doi: 10.1016/j.rser.2013.05.063.
[25] R. J. Geider, H. L. MacIntyre, et T. M. Kana, « A dynamic regulatoy model of phytoplankton acclimation to light, nutrients, and temperature », *Limnol. Oceanogr. J. Mar. Syst.*, vol. 43, n° 4, p. 679-694, 1998.
[26] B. W. Bequette, « software package, including the S », n° December 2001, p. 3-7, 2003.
[27] Q. Béchet, A. Shilton, J. B. K. Park, R. J. Craggs, et B. Guieysse, « Universal Temperature Model for Shallow Algal Ponds Provides Improved Accuracy », *Environ. Sci. Technol.*, vol. 45, n° 8, p. 3702-3709, avr. 2011, doi: 10.1021/es1040706.
[28] P. M. Slegers, R. H. Wijffels, G. van Straten, et A. J. B. van Boxtel, « Design scenarios for flat panel photobioreactors », *Appl. Energy*, vol. 88, n° 10, p. 3342-3353, 2011, doi: 10.1016/j.apenergy.2010.12.037.
[29] Q. Béchet, A. Shilton, et B. Guieysse, « Modeling the effects of light and temperature on algae growth: State of the art and critical assessment for productivity prediction during outdoor cultivation », *Biotechnol. Adv.*, vol. 31, n° 8, p. 1648-1663, 2013, doi: 10.1016/j.biotechadv.2013.08.014.
[30] J. C. Goldman et E. J. Carpenter, « A kinetic approach to the effect of temperature on algal growth », *Limnol. Oceanogr.*, vol. 19, n° 5, p. 756-766, 1974.
[31] E. Rodríguez-Miranda, F. G. Acién, J. L. Guzmán, M. Berenguel, et A. Visioli, « A new model to analyze the temperature effect on the microalgae performance at large scale raceway reactors », *Biotechnol. Bioeng.*, vol. 118, n° 2, p. 877-889, févr. 2021, doi: 10.1002/bit.27617.
[32] E. Rodríguez-Miranda, J. L. Guzmán, F. G. Acién, M. Berenguel, et A. Visioli, « Indirect regulation of temperature in raceway reactors by optimal management of culture depth », *Biotechnol. Bioeng.*, vol. 118, n° 3, p. 1186-1198, mars 2021, doi: 10.1002/bit.27642.
[33] C. Posten, « Design principles of photo-bioreactors for cultivation of microalgae », *Eng. Life Sci.*, vol. 9, n° 3, p. 165-177, 2009, doi: 10.1002/elsc.200900003.
[34] H. Luoheng et D. C. Rundquist, « Comparison of NIR/RED ratio and first derivative of reflectance in estimating algal-chlorophyll concentration: A case study in a turbid reservoir », *Remote Sens. Environ.*, vol. 62, n° 3, p. 253-261, 1997, doi: 10.1016/S0034-4257(97)00106-5.
[35] A. Solovchenko, I. Khozin-Goldberg, L. Recht, et S. Boussiba, « Stress-Induced Changes in Optical Properties, Pigment and Fatty Acid Content of Nannochloropsis sp.: Implications for Non-

destructive Assay of Total Fatty Acids », *Mar. Biotechnol.*, vol. 13, n° 3, p. 527-535, 2011, doi: 10.1007/s10126-010-9323-x.
[36] R. A. Andersen, *Algal Culturing Techniques*. 2005. doi: 10.1111/j.1529-8817.2005.00114.x.
[37] J. R. Welty, C. E. Wicks, R. E. Wilson, et G. L. Rorrer, *Fundamentals of momentum, heat and mass transfer*, 5th éd. 2000. doi: 10.1016/0017-9310(70)90063-3.
[38] S. Churchill et H. Chu, « Correlating equations for laminar and turbulent free convection from a vertical plate », *Int. J. Heat Mass Transf.*, vol. 18, n° 11, p. 1323-1329, 1875.
[39] J. A. Palyvos, « A survey of wind convection coefficient correlations for building envelope energy systems' modeling », *Appl. Therm. Eng.*, vol. 28, n° 8-9, p. 801-808, 2008, doi: 10.1016/j.applthermaleng.2007.12.005.
[40] Meteonorm, « Meteonorm: Irradiation data for every place on Earth », 2017. http://www.meteonorm.com/ (consulté le 23 juin 2018).
[41] H. V. Gupta, H. Kling, K. K. Yilmaz, et G. F. Martinez, « Decomposition of the mean squared error and NSE performance criteria: Implications for improving hydrological modelling », *J. Hydrol.*, vol. 377, n° 1-2, p. 80-91, 2009, doi: 10.1016/j.jhydrol.2009.08.003.
[42] E. Nash et V. Sutcliffe, « PART I- A DISCUSSION OF PRINCIPLES * The problem of determining river flows from rainfall , evaporation , and other factors , occupies a central place in the technology of applied hydrology . It is not only the essential problem of flood forecasting but a », vol. 10, p. 282-290, 1970.
[43] J. E. Nash et J. V. Sutcliffe, « River flow forecasting through conceptual models part I — A discussion of principles », *J. Hydrol.*, vol. 10, n° 3, p. 282-290, avr. 1970, doi: 10.1016/0022-1694(70)90255-6.
[44] A. Ritter et R. Muñoz-Carpena, « Performance evaluation of hydrological models: Statistical significance for reducing subjectivity in goodness-of-fit assessments », *J. Hydrol.*, vol. 480, p. 33-45, févr. 2013, doi: 10.1016/J.JHYDROL.2012.12.004.
[45] D. N. Moriasi, J. G. Arnold, M. W. Van Liew, R. L. Bingner, R. D. Harmel, et T. L. Veith, « Model Evaluation Guidelines for Systematic Quantification of Accuracy in Watershed Simulations », vol. 50, n° 3, p. 885-900, 2007.

A dynamic model for temperature prediction in a façade-integrated photobioreactor

Integration of PBR to building façade as a promising way to reduce energy consumption of microalgae culture process

Integration of PBR to building :
Industrial ecology
Waste recycling

Pilot-scale study

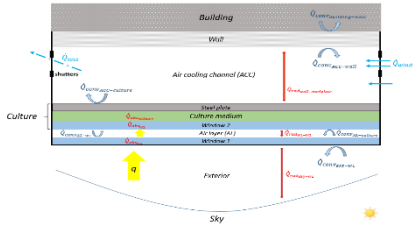

Thermal modelling

experimental validation

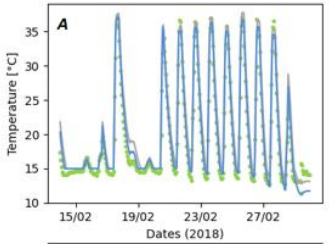

Model based design

Temperature control strategy

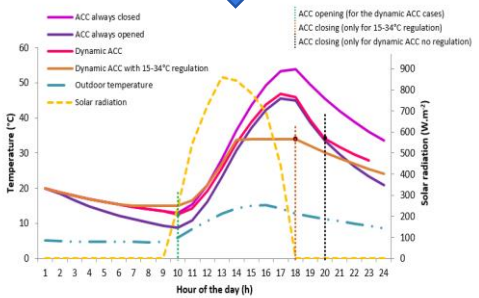

Energy savings

Saint-Nazaire, France

Nantes Université, Oniris, CNRS, GEPEA

Funder :
FUI SYMBIO2 project